



Bayesian inference of the specific shear and bulk viscosities of the quark-gluon plasma at crossover from ϕ and Ω observables

Zhidong Yang  and Lie-Wen Chen *

School of Physics and Astronomy, Shanghai Key Laboratory for Particle Physics and Cosmology, and Key Laboratory for Particle Astrophysics and Cosmology (MOE), Shanghai Jiao Tong University, Shanghai 200240, China



(Received 3 August 2022; revised 19 May 2023; accepted 14 June 2023; published 26 June 2023)

Due to their weak final state interactions, the ϕ meson and Ω baryon provide unique probes of the properties of the quark-gluon plasma (QGP) formed in relativistic heavy-ion collisions. Using the quark recombination model with the quark phase-space information parametrized in a viscous blast wave, we study the transverse-momentum spectra and elliptic flows of ϕ and Ω in Au + Au collisions at $\sqrt{s_{NN}} = 200$ GeV and Pb + Pb collisions at $\sqrt{s_{NN}} = 2.76$ TeV. The viscous blast wave includes nonequilibrium deformations of thermal distributions due to shear and bulk stresses and thus carries information on the specific shear viscosity η/s and the specific bulk viscosity ζ/s of the QGP. We perform a model-to-data comparison with Bayesian inference and simultaneously obtain $\eta/s = (2.08_{-1.09}^{+1.10})/4\pi$ and $\zeta/s = 0.06_{-0.04}^{+0.04}$ at 90% C.L. for the baryon-free QGP at crossover temperature of about 160 MeV. Our work provides a unique approach to simultaneously determine the η/s and ζ/s of the QGP at hadronization.

DOI: [10.1103/PhysRevC.107.064910](https://doi.org/10.1103/PhysRevC.107.064910)

I. INTRODUCTION

A new state of matter that consists of deconfined quarks and gluons, called the quark-gluon plasma (QGP), is believed to have been created in relativistic heavy-ion collisions (HICs) at the BNL Relativistic Heavy Ion Collider (RHIC) and the CERN Large Hadron Collider (LHC). The QGP is expected to fill the early universe at about 10^{-6} s after the big bang. Studies show that the QGP behaves like a near-perfect fluid and has very small specific shear viscosity η/s [1,2], i.e., the ratio of shear viscosity η to entropy density s , close to the universal lower bound $\eta/s = 1/4\pi$ based on the anti de Sitter-conformal field theory (AdS/CFT) correspondence [3]. It turns out that the η/s directly characterizes the behavior of QGP fluid and has significant impacts on the final observables of HICs. Studies also indicate the bulk viscosity (ζ) has non-negligible effects on HIC observables [4,5].

Determining the temperature and baryon density dependence of QGP's η/s and ζ/s is of fundamental importance and remains a big challenge in the field [6]. For zero baryon density or baryon chemical potential ($\mu_B = 0$), the first principle lattice quantum chromodynamics (LQCD) predicts that the transition from hadrons to QGP is not a real phase transition but a smooth crossover at a pseudocritical temperature $T_{pc} \approx 160$ MeV [7,8]. Theoretical calculations on the temperature dependence of the viscosities of the baryon-free QGP have been widely explored in various approaches in the past years, including LQCD [9–13], functional renormalization group (FRG) method [14], T matrix [15], and perturbative QCD (pQCD) [16] for the η/s , as well as LQCD

[17–19] and holographic model [20] for the ζ/s . Overall, the theoretical predictions remain largely uncertain even at T_{pc} and the first principle calculation is still challenging [21]. Alternately, many efforts have focused on constraining the viscosities of QGP with experimental observables.

Early works using viscous hydrodynamics have given semiquantitative estimates on the η/s of QGP [1,22–24]. Usually they assumed a constant η/s over the entire evolution and found $\eta/s = 1 \sim 2.5/(4\pi)$. Recently, results using multistage approaches which combine initial conditions, viscous hydrodynamics, and hadronic transport are reported in Refs. [25–35]. A variety of experimental observables, often focused on protons, kaons, and pions, and a number of parameters are used in these works. Although they used very similar methods, the obtained results tend to be different, depending on the details of the model and observables. For example, for the baryon-free QGP at T_{pc} , the JETSCAPE Collaboration reported $\eta/s \approx 1.6/(4\pi)$ and $\zeta/s \approx 0.09$ [28], while the Trajectum group reported $\eta/s \approx 0.9/(4\pi)$ and $\zeta/s \approx 0.004$ [30], displaying a significant discrepancy. Very recently the Trajectum group updated their results to $\eta/s \approx 2.3/(4\pi)$ and $\zeta/s \approx 0.02$ at T_{pc} after considering the recent measured nucleon nucleon cross section [32]. Meanwhile, they reported $\eta/s(T)$ decreases as temperature increases [32], which is opposite to the results of the Duke group [27].

In this work, we present a unique approach to constrain the η/s and ζ/s of the baryon-free QGP at T_{pc} by using the measured transverse-momentum spectra and elliptic flows of ϕ and Ω in Au + Au collisions at $\sqrt{s_{NN}} = 200$ GeV and Pb + Pb collisions at $\sqrt{s_{NN}} = 2.76$ TeV where the QGP has a negligible baryon density and its transition to hadrons is a smooth crossover. In our approach, hadrons are produced through quark recombination [36–41] with the phase-space distribu-

*Corresponding author: lwchen@sjtu.edu.cn

tion of quarks at hadronization parametrized in a viscous blast wave [42–46] which includes nonequilibrium deformations of thermal distributions due to shear and bulk stresses. The viscous corrections on the QGP at hadronization are then imported into ϕ and Ω through the recombination process. Since the ϕ and Ω have weak hadronic interactions [47], they thus carry direct information of QGP at hadronization with negligible hadronic effects [47–55], making it possible to determine the η/s and ζ/s of the QGP at crossover from the ϕ and Ω observables.

II. MODEL AND METHODS

A. Theoretical model

Quark recombination or coalescence models were first proposed to explain the baryon-over-meson enhancement and valence quark number scaling in RHIC Au + Au collisions [36–39]. In these models, valence quarks are assumed to be abundant in the phase space and recombine into hadrons through quark recombination. The hadron formation process is usually assumed to be instantaneous and takes a very thin hypersurface ($\Delta\tau \approx 0$). Following Refs. [38–40], the momentum distribution of baryons is given by

$$E \frac{dN_B}{d^3\mathbf{p}} = C_B \int_{\Sigma} \frac{p^\mu \cdot d\sigma_\mu}{(2\pi)^3} \int_0^1 dx_1 dx_2 dx_3 \Phi_B(x_1, x_2, x_3) \times f_a(\mathbf{r}, x_1 \mathbf{p}) f_b(\mathbf{r}, x_2 \mathbf{p}) f_c(\mathbf{r}, x_3 \mathbf{p}), \quad (1)$$

where C_B is the spin degeneracy factor of a given baryon species, Σ is the hypersurface of hadronization, Φ_B is the effective wave function squared of baryons, $x_{1,2,3}$ are light cone coordinates defined as $\mathbf{p}_{1,2,3} = x_{1,2,3} \mathbf{p}$, and $f_{a,b,c}$ are the parton phase-space distributions. Here, we make the assumption that the partons are essentially ultrarelativistic and traveling along the light cone, which should be valid for the LHC and the top RHIC energies. The Φ_B is parametrized as polynomial [39], and here we use a Gaussian ansatz $\Phi_B \sim \exp(-\frac{(x_1-x_a)^2+(x_2-x_b)^2+(x_3-x_c)^2}{\sigma_B^2}) \delta(x_1+x_2+x_3-1)$, where $x_{a,b,c} = m_{1,2,3}/(m_1+m_2+m_3)$ are the peak values, and $m_{1,2,3}$ are the masses of the constitute partons. Similar expression can be derived for mesons.

The quark phase-space distribution is parametrized in a viscous blast wave [44–46], based on a Retiere and Lisa (RL) blast wave [56]. The quark distribution is given by

$$f(r, p) = f_0(r, p) + \delta f_{\text{shear}}(r, p) + \delta f_{\text{bulk}}(r, p), \quad (2)$$

where f_0 is the equilibrium Bose/Fermi distribution, δf_{shear} and δf_{bulk} are corrections from the shear and bulk viscosities, respectively. For the shear viscous corrections, we use Grad's method [2,57]

$$\delta f_{\text{shear}} = \frac{1}{2s} \frac{p^\mu p^\nu}{T^3} \pi^{\mu\nu} f_0(1 \pm f_0), \quad (3)$$

where $\pi^{\mu\nu}$ is the shear stress tensor and $+$ ($-$) for bosons (fermions). In the Navier-Stokes approximation $\pi^{\mu\nu} = 2\eta\sigma^{\mu\nu}$, where $\sigma^{\mu\nu}$ is the shear gradient tensor defined as $\sigma^{\mu\nu} = \frac{1}{2}(\nabla^\mu u^\nu + \nabla^\nu u^\mu) - \frac{1}{3}\Delta^{\mu\nu}\nabla_\lambda u^\lambda$ with flow field u^μ , $\nabla^\mu = \Delta^{\mu\nu}\partial_\nu$, and $\Delta^{\mu\nu} = g^{\mu\nu} - u^\mu u^\nu$. For the bulk viscous

corrections, we use the 14-moment approximation [58,59]

$$\delta f_{\text{bulk}} = -f_0(1 \pm f_0) \Pi \frac{\tau_\Pi}{\zeta} \left[\frac{1}{3} \frac{m^2}{T} \frac{1}{p^\mu u_\mu} + \frac{p^\mu u_\mu}{T} \left(c_s^2 - \frac{1}{3} \right) \right], \quad (4)$$

where Π is the bulk viscous pressure and τ_Π is the bulk relaxation time. At the first order approximation, one has $\Pi = -\zeta \partial_\mu u^\mu$. The expression for $\frac{\tau_\Pi}{\zeta}$ is given in [58].

Now we present the blast wave parametrization for the flow field u^μ . In the following, $R_{x,y}$ are the semiaxes of the fireball at freeze-out, $\rho = \sqrt{x^2/R_x^2 + y^2/R_y^2}$ is the reduced radius, $\eta_s = \frac{1}{2} \log \frac{t+z}{t-z}$ is the space-time rapidity. The hypersurface is assumed to be constant $\tau = \sqrt{t^2 - z^2}$. The flow field is parametrized as

$$u^\mu = (\cosh \eta_s \cosh \eta_T, \sinh \eta_T \cos \phi_b, \sinh \eta_T \sin \phi_b, \sinh \eta_s \cosh \eta_T), \quad (5)$$

where η_T is the transverse flow rapidity and ϕ_b is the azimuthal angle of u^μ in the transverse plane. Here, we assume boost invariance and set longitudinal flow rapidity to be equal to the space-time rapidity η_s . η_T is given by the transverse velocity $v_T = \tanh \eta_T$ with

$$v_T = \rho^n (\alpha_0 + \alpha_2 \cos 2\phi_b), \quad (6)$$

where α_0 is the average surface velocity, α_2 is an elliptic deformation of the flow field, and n is a power term. In this work, we use a linear expression and set $n = 1$. We choose the transverse flow vector perpendicular to the elliptic surface at $\rho = 1$, i.e., $\tan \phi_b = R_x^2/R_y^2 \tan \phi$, where $\phi = \arctan y/x$ is the azimuthal angle of the position. In terms of the geometric parameters, it turns out the ratio R_y/R_x has a large influence on elliptical flow, so we choose R_y/R_x as a fit parameter and constrain R_x , R_y , and τ by fitting the ratio R_y/R_x and by adding the simple geometric estimate $R_x \approx (R_0 - b/2) + \tau c_\tau (\alpha_0 + \alpha_2)$, where R_0 is the radius of the colliding nucleus, b is the impact parameter, and $c_\tau = \bar{\alpha}_0/\alpha_0$ relates the time-averaged surface velocity. In this work we use $R_0 = 7.1$ fm (7.0 fm) for Pb (Au) based on formula in [60] and $c_\tau = 0.65$. The values of b for each centrality bin are taken from Glauber Monte Carlo simulations used by related experiments [61,62].

It should be noted that the viscous blast wave parametrizes the flow field and freeze-out hypersurface with a simple ansatz, which can be regarded as an approximate snapshot of a viscous hydrodynamic system at a fixed time [42–46]. Therefore, the viscous blast wave carries information on the viscosities of the fluid at a fixed time, e.g., the QGP at hadronization in our present work.

B. Experimental data and fit parameters

To compare our model to experiment, we utilize the transverse-momentum (p_T) spectra and elliptic flows v_2 of ϕ and Ω as our observables. The data are taken from the STAR Collaboration for Au + Au collisions at $\sqrt{s_{NN}} = 200$ GeV [63–65] and the ALICE Collaboration for Pb + Pb collisions at $\sqrt{s_{NN}} = 2.76$ TeV [66–68] at midrapidity. For v_2

of ϕ and Ω , we use the data in centralities 0–30 %, 30–80 % from STAR, and 10–20 %, 20–30 %, 30–40 %, 40–50 % from ALICE. Due to the limit of available data, the centrality bins for p_T spectra are slightly different from that of v_2 . For the ϕ spectra, we use the data in 10–20 %, 40–50 % from STAR and 10–20 %, 20–30 %, 30–40 %, 40–50 % from ALICE. For the Ω spectra, we use the data in 0–5 % and 40–60 % from STAR and 10–20 %, 20–40 %, 40–60 % from ALICE. When the centrality of spectra are not matched to that of v_2 , we choose the spectra that belongs to the neighbor centrality.

The fit ranges are $p_T < 1.8$ GeV/ c for ϕ and $p_T < 3.2$ GeV/ c for Ω . We do a combined analysis for both STAR and ALICE data and have 116 data points in total. We note that the correction $\delta f(r, p)$ is small for both ϕ and Ω , i.e., less than 20% of f_0 for the majority of points (very few points up to 40% of f_0), which is much smaller than the usually adopted upper bound ~ 1 [29,42], guaranteeing the applicability of the viscous corrections.

The parameters entering the model are $(\tau, T, \alpha_0, \alpha_2, R_y/R_x, \eta/s, \zeta/s)$ from the blast wave and (σ_B, σ_M) from the quark recombination. Here, $\sigma_B(\sigma_M)$ is the wave function width for baryons (mesons). We find the values of $\sigma_{M,B}$ mainly affect the particle yields and have little impact on v_2 . To describe the yields of ϕ and Ω , we set $\sigma_M = 0.3$, $\sigma_B = 0.09$. We note that our conclusion changes little by varying the values of σ_M and σ_B . The freeze-out or recombination hypersurface is related to the fireball volume and can be determined from the particle yield.

For the other constants, we use sound speed squared $c_s^2 = 0.15$ [see Eq. (4)] for the baryon-free QGP at T_{pc} [69], quark mass $m_s = 0.5$ GeV, spin degeneracy factor $C_M = 3$ for ϕ , and $C_B = 4$ for Ω^- (or $\bar{\Omega}^+$). To fit the yield of ϕ and Ω as well as determine the value of freeze-out time τ , we introduce a fugacity factor $\gamma_{s,\bar{s}}$ for strange quarks and set $\gamma_{s,\bar{s}} = 0.8$ for all centrality bins which is close to the value found in [54]. Now the parameters left in our model are $(T, \alpha_0, \alpha_2, R_y/R_x, \eta/s, \zeta/s)$. For each centrality bin of STAR (0–30 %, 30–80 %) and ALICE (10–20 %, 20–30 %, 30–40 %, 40–50 %), the fluid has unique values for α_0, α_2 , and R_y/R_x with the same shared values for $T, \eta/s$, and ζ/s , and thus we have 21 parameters.

C. Bayesian method

To determine the above parameters, we use the Bayesian analysis package from the models and data analysis initiative (MADAI) project [26,70]. The MADAI package includes a Gaussian process emulator and a Bayesian analysis tool. According to Bayes' theorem, for model parameters $x = (x_1, x_2, x_3, \dots)$ and experimental observables $y = (y_1, y_2, y_3, \dots)$, the probability for the true parameters x_* is

$$P(x_*|X, Y, y_{\text{exp}}) \propto P(X, Y, y_{\text{exp}}|x_*)P(x_*). \quad (7)$$

The left-hand side is the *posterior* probability of x_* given the design (X, Y) and the experimental data y_{exp} . On the right-hand side, $P(x_*)$ is the *prior* probability and $P(X, Y, y_{\text{exp}}|x_*)$ is the *likelihood*, i.e., the probability of the

model describing the data y_{exp} at x_* , given by

$$P(X, Y, y_{\text{exp}}|x_*) \propto \exp\left(-\frac{1}{2}\Delta y^\top \Lambda^{-1} \Delta y\right), \quad (8)$$

where $\Delta y = y_* - y_{\text{exp}}$ is the difference between the measurement and the prediction, and Λ is the covariance matrix including the experimental and model uncertainties. More details can be found in [26,29].

All model parameters have *uniform* prior distribution except for the recombination temperature T , which has a *Gaussian* prior. For example, we use prior ranges 0–4.4/(4 π) for η/s , 0–0.16 for ζ/s , and 0.72–0.8 c for α_0 , 0.02–0.036 c for α_2 , 1.1–1.18 for R_y/R_x in 0–30 % centrality bin of STAR. For T , we use a Gaussian distribution with a mean value of 160 MeV and a standard deviation of 5 MeV to reflect our prior knowledge of quark recombination temperature of a continuous crossover at $T_{pc} = 158 \pm 15$ MeV for zero net baryon density [8].

The Bayesian analysis package works as follows. First, we set prior ranges for each parameter and generate a set of training points in the parameter space. Second, we calculate all fitted observables at each training point. The package then builds a Gaussian process emulator, which can estimate the observables for random parameter values. Finally a Markov chain Monte Carlo (MCMC) provides a likelihood analysis and gives the maximum likelihood or best-fit parameters. Here, we have 21 parameters and use $N = 500$ training points. To verify the Bayesian analysis works properly, we perform a validation for the Bayesian inference framework and find the Bayesian framework correctly reproduces model parameters within reasonable uncertainties. The likelihood analysis has used $N_* = 10^7$ predicted points to search for the best-fit parameters, which is sufficient for MCMC to converge.

III. RESULTS AND DISCUSSIONS

Using the data and prior parameter ranges, we perform a model-to-data comparison with the MADAI package. Figure 1 shows the univariate posterior distributions for the recombination temperature T , η/s , and ζ/s . We obtain $T = 159 \pm 8$ MeV, $\eta/s = (2.08_{-1.09}^{+1.10})/4\pi$, and $\zeta/s = 0.06_{-0.04}^{+0.04}$ at 90% confidence level (C.L.). Figure 1 also shows the correlations between T , η/s , and ζ/s . We find there is a strong correlation between η/s and ζ/s . This can be qualitatively understood by the different effects of η/s and ζ/s on the particle momentum distribution, i.e., the η/s decreases the azimuthal momentum asymmetry of particles, while the ζ/s reduces their momenta isotropically [28]. As a result, the ζ/s tends to increase v_2 while the η/s prefers to reduces v_2 at higher p_T . We also find there is a slight anticorrelation between T and η/s , and a moderate correlation between T and ζ/s .

For the other parameters, we show the best-fit values, which are defined as the mean value given by maximum likelihood analysis, as given in Table I. Using the best-fit parameters, we calculate the p_T spectra and v_2 of ϕ and Ω and compare them with data. Figure 2 shows the results of p_T spectra and v_2 in different centrality bins for Au + Au collisions at $\sqrt{s_{NN}} = 200$ GeV and Pb + Pb at $\sqrt{s_{NN}} = 2.76$ TeV,

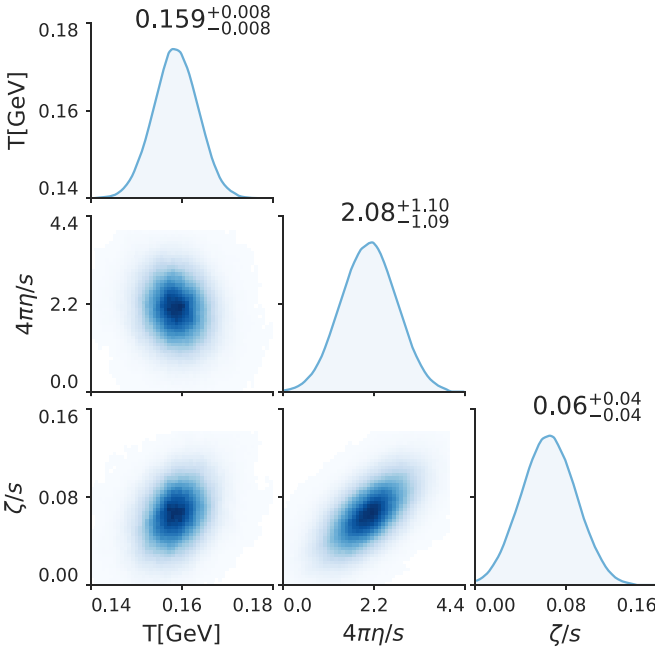


FIG. 1. Posterior distributions and correlations of selected parameters: T , η/s , and ζ/s . The numbers indicate the median values with the 90%-credibility range.

respectively. As expected, our calculations describe the data rather well.

Figure 3 shows our Bayesian inference of the η/s and ζ/s for the baryon-free QGP at $T_{pc} \approx 160$ MeV (with 68.3% and 90% C.L., indicated by SJTU). For comparison, we include in Fig. 3(a) the temperature dependence of η/s for the baryon-free QGP/hadronic matter from other approaches, i.e., the multistage methods (with 90% C.L.) from Duke [27], JETSCAPE [28], and Trajectum [32], the viscous blast wave (BW) [46], Chapman-Enskog (Chap-Ensk) method [71], hadron resonance gas (HRG) model with Hagedorn states (HS) [72], FRG [14], LQCD (Lattice1 [9,10], Lattice2 [11], Lattice3 [12], and Lattice4 [13], with 68.3% C.L.), T matrix [15], and next-to-leading order pQCD [16]. Similarly, Fig. 3(b) includes the corresponding results for ζ/s from the multistage methods from Duke [27], JETSCAPE [28], and Trajectum [32], LQCD (Lattice1 [18], Lattice3 [19], and

TABLE I. The best-fit values of the viscous blast wave parameters for different centrality bins with $T = 159$ MeV, $\eta/s = 2.08/(4\pi)$, and $\zeta/s = 0.06$.

Centrality	τ (fm/c)	$\alpha_0(c)$	$\alpha_2(c)$	R_y/R_x
Au+Au 200 GeV				
0–30 %	7.8	0.76	0.027	1.13
30–80 %	5.1	0.70	0.039	1.31
Pb+Pb 2.76 TeV				
10–20 %	9.4	0.84	0.028	1.18
20–30 %	9	0.81	0.037	1.18
30–40 %	7.8	0.81	0.036	1.25
40–50 %	6.8	0.79	0.031	1.36

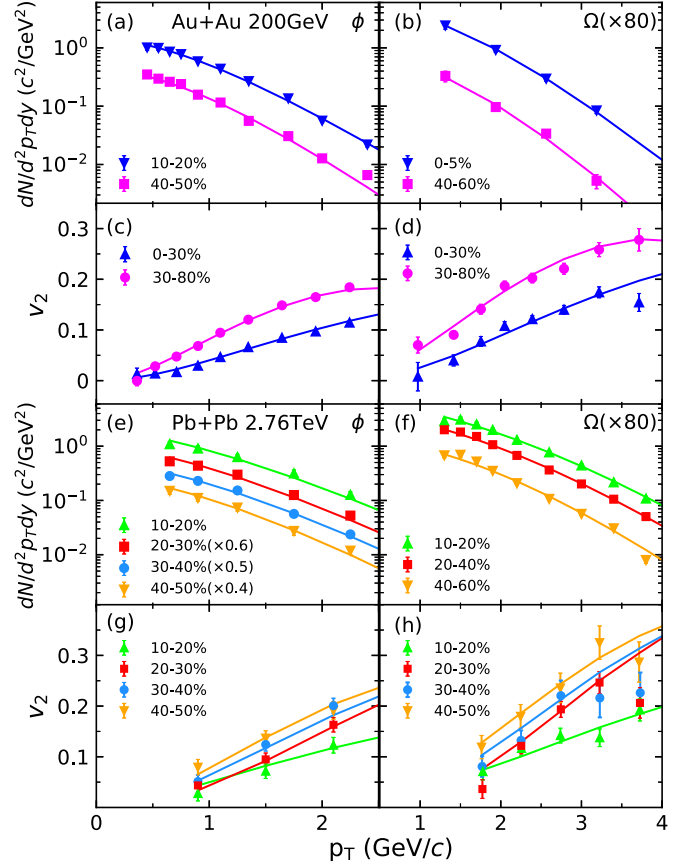


FIG. 2. Transverse-momentum spectra and elliptic flows v_2 of ϕ and $\Omega^- + \bar{\Omega}^+$ at midrapidity in Au + Au collisions at $\sqrt{s_{NN}} = 200$ GeV and Pb + Pb collisions at $\sqrt{s_{NN}} = 2.76$ TeV from the recombination model using the best-fit parameters given by Bayesian analysis. The data from STAR [63–65] and ALICE [66–68] are included for comparison.

Lattice5 [17], with 68.3% C.L.), hybrid model (McGill) [4], holographic model (Holo) [20], HRG model with HS [72], and SMASH transport model [73].

It is interesting to see from Fig. 3(a) that different methods give roughly consistent results for η/s , indicating a trend that the η/s approaches a minimum at the crossover temperature T_{pc} , with a rather steep rise towards lower temperatures and a slow rise towards higher temperatures. The behavior with minimum η/s at T_{pc} is also observed in recent work based on a $2 + 1$ dimensional hydrodynamical model with the Eskola-Kajantie-Ruuskanen-Tuominen (EKRT) initial state [74] and the quasiparticle model prediction [75]. We note our present constraint on the η/s at T_{pc} is compatible with those of Duke, JETSCAPE, and Trajectum from the multistage methods, as well as the Chap-Ensk, BW, FRG, and Lattice3.

On the other side, one sees from Fig. 3(b) that the results of ζ/s exhibit significant discrepancy around T_{pc} . For example, at T_{pc} , a rather large value of $\zeta/s \approx 0.35$ is obtained from the LQCD (Lattice3 and Lattice5) and McGill group, $\zeta/s \approx 0.09$ from JETSCAPE, $\zeta/s \approx 0.06$ from our present work, $\zeta/s \approx 0.03$ from Duke group, and $\zeta/s \approx 0.02$ from Trajectum. In general, our result on ζ/s is in good agreement

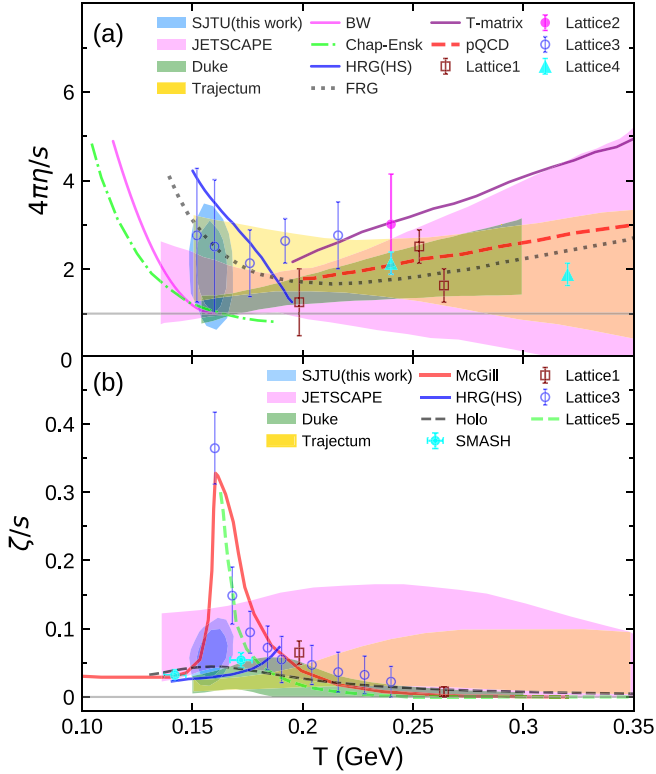


FIG. 3. Temperature dependence of η/s (a) and ζ/s (b) for QGP/hadronic matter at $\mu_B = 0$ (see text for details).

with those from the holographic model, SMASH transport model, and JETSCAPE, and has minor overlap with that from Duke and Trajectum. The discrepancies between Duke, JETSCAPE, and Trajectum mainly come from different treatments of observations and parameters [30] although they use the similar multistage methods. The ζ/s is believed to have a peak around T_{pc} and go to zero at sufficiently high temperatures [4, 17, 29], while the magnitude of the peak value remains unknown and depends on the model [6].

We note that using higher p_T ranges of experimental data has a minor influence on our results. For example, using $p_T < 2.3 \text{ GeV}/c$ for ϕ mesons and $p_T < 3.6 \text{ GeV}/c$ for Ω baryons leads to $T = 160 \pm 8 \text{ MeV}$, $4\pi\eta/s = 2.14 \pm 0.44$, and $\zeta/s = 0.04 \pm 0.03$ at 90% C.L. As expected, the higher p_T ranges have more data points and put stronger constraints on η/s and ζ/s . On the other hand, the higher p_T ranges will cause larger viscous corrections for f_0 , and the threshold of applicable p_T is not known precisely. Since using higher p_T ranges is at risk to violate the applicability of the model, we make a conservative choice and use lower ranges in this work. We look forward to using more precise data from future experimental measurements to reduce the uncertainties.

We now discuss the uncertainties in our analysis. In general, we can group them into three categories: (a) Uncertainties from assumptions made in blast wave parametrization, e.g., the simple ansatz for the flow field and the recombine hypersurface, and the Navier-Stokes approximation for shear stress. (b) Uncertainties from assumptions made in quark

recombination formalism, e.g., the instantaneous hadronization process and simple form for wave function squared of hadrons. (c) Uncertainties from the errors in experimental data and the quality of the Gaussian emulator. To quantify uncertainty (a), one can compare hydro simulations with blast wave, which is what we did in [45]. We find the uncertainties ($\approx 0.1/4\pi$) from approximations used in the blast wave is rather small compared with uncertainties from Bayesian analysis ($\approx 1/4\pi$). To give a rough estimate for uncertainty (b), we vary the wave function width of mesons and baryons by increasing their values by 33%, i.e., from the default $\sigma_M = 0.3$ and $\sigma_B = 0.09$ to $\sigma_M = 0.4$ and $\sigma_B = 0.12$, and we obtain $\eta/s = 2.0/4\pi$ and $\zeta/s = 0.07$, which correspond to minor changes, i.e., a decrease of η/s by 4% and an increase of ζ/s by 8%. We note that for uncertainty (c), one could use a more refined recombination formula, such as the formula in [54] to decrease the uncertainty. Uncertainty (c) is provided by the MADAI code and is shown in our final results. In addition, there could be uncertainties from the assumption that ϕ and Ω have weak hadronic interactions. In principle, a quantitative estimate of the uncertainties could be obtained by including hadronic transport simulations after hadronization, but this is beyond the scope of the present work and it would be interesting to pursue in future.

Finally, we would like to mention that in the present work, the quark phase-space distribution is parametrized by a viscous blast wave and the η/s and ζ/s of the QGP are only constrained at crossover. An alternative and perhaps more realistic way is to take the phase-space distribution of quarks from viscous hydrodynamic simulations, which can include parametrized $\eta/s(T)$ and $\zeta/s(T)$ of the QGP. By doing this, one may extract information on the temperature dependence of the η/s and ζ/s of the QGP from the ϕ and Ω observables. Such a hybrid approach combining a hydrodynamic model and quark recombination has been recently proposed in Ref. [76], and in the future, we may follow the similar approach to investigate the η/s and ζ/s of the QGP from the ϕ and Ω observables.

IV. CONCLUSIONS

Within the quark recombination model with the quark phase-space distribution parametrized in a viscous blast wave, we have demonstrated that the ϕ and Ω produced in relativistic heavy-ion collisions can be used to constrain the specific shear viscosity η/s and the specific bulk viscosity ζ/s of the QGP at hadronization. By performing Bayesian analyses on the measured transverse-momentum spectra and elliptic flows of ϕ and Ω in Au + Au collisions at $\sqrt{s_{NN}} = 200 \text{ GeV}$ and Pb + Pb collisions at $\sqrt{s_{NN}} = 2.76 \text{ TeV}$, we obtain $\eta/s = (2.08^{+1.10}_{-1.09})/4\pi$ and $\zeta/s = 0.06^{+0.04}_{-0.04}$ at 90% C.L. for the baryon-free QGP at crossover temperature $T_{pc} \approx 160 \text{ MeV}$. Our work suggests that high quality data of ϕ and Ω in heavy-ion collisions at various energies may provide important information on the temperature and baryon density dependence of QGP's η/s and ζ/s .

ACKNOWLEDGMENTS

The authors would like to thank Rainer J. Fries, Guang-You Qin, and Yifeng Sun for useful discussions. This work

was supported by the National Natural Science Foundation of China under Grants No. 12205182, No. 12235010, and No. 11625521, and the National SKA Program of China Grant No. 2020SKA0120300.

-
- [1] P. Romatschke and U. Romatschke, *Phys. Rev. Lett.* **99**, 172301 (2007).
- [2] H. Song and U. W. Heinz, *Phys. Rev. C* **77**, 064901 (2008).
- [3] P. K. Kovtun, D. T. Son, and A. O. Starinets, *Phys. Rev. Lett.* **94**, 111601 (2005).
- [4] S. Ryu, J. F. Paquet, C. Shen, G. S. Denicol, B. Schenke, S. Jeon, and C. Gale, *Phys. Rev. Lett.* **115**, 132301 (2015).
- [5] S. Ryu, J.-F. Paquet, C. Shen, G. Denicol, B. Schenke, S. Jeon, and C. Gale, *Phys. Rev. C* **97**, 034910 (2018).
- [6] C. Shen, *Nucl. Phys. A* **1005**, 121788 (2021).
- [7] T. Bhattacharya *et al.*, *Phys. Rev. Lett.* **113**, 082001 (2014).
- [8] S. Borsanyi, Z. Fodor, J. N. Guenther, R. Kara, S. D. Katz, P. Parotto, A. Pasztor, C. Ratti, and K. K. Szabo, *Phys. Rev. Lett.* **125**, 052001 (2020).
- [9] H. B. Meyer, *Phys. Rev. D* **76**, 101701(R) (2007).
- [10] H. B. Meyer, *Nucl. Phys. A* **830**, 641c (2009).
- [11] S. W. Mages, S. Borsanyi, Z. Fodor, A. Schäfer, and K. Szabó, *PoS LATTICE2014*, 232 (2015).
- [12] N. Astrakhantsev, V. Braguta, and A. Kotov, *J. High Energy Phys.* **04** (2017) 101.
- [13] S. Borsanyi, Z. Fodor, M. Giordano, S. D. Katz, A. Pasztor, C. Ratti, A. Schafer, K. K. Szabo, and B. C. Tóth, *Phys. Rev. D* **98**, 014512 (2018).
- [14] N. Christiansen, M. Haas, J. M. Pawłowski, and N. Strodthoff, *Phys. Rev. Lett.* **115**, 112002 (2015).
- [15] S. Y. F. Liu and R. Rapp, *Eur. Phys. J. A* **56**, 44 (2020).
- [16] J. Ghiglieri, G. D. Moore, and D. Teaney, *J. High Energy Phys.* **03** (2018) 179.
- [17] F. Karsch, D. Kharzeev, and K. Tuchin, *Phys. Lett. B* **663**, 217 (2008).
- [18] H. B. Meyer, *Phys. Rev. Lett.* **100**, 162001 (2008).
- [19] N. Y. Astrakhantsev, V. V. Braguta, and A. Y. Kotov, *Phys. Rev. D* **98**, 054515 (2018).
- [20] R. Rougemont, R. Critelli, J. Noronha-Hostler, J. Noronha, and C. Ratti, *Phys. Rev. D* **96**, 014032 (2017).
- [21] G. D. Moore, [arXiv:2010.15704](https://arxiv.org/abs/2010.15704).
- [22] B. Schenke, S. Jeon, and C. Gale, *Phys. Rev. Lett.* **106**, 042301 (2011).
- [23] C. Gale, S. Jeon, B. Schenke, P. Tribedy, and R. Venugopalan, *Phys. Rev. Lett.* **110**, 012302 (2013).
- [24] H. Niemi, K. J. Eskola, and R. Paatelainen, *Phys. Rev. C* **93**, 024907 (2016).
- [25] J. E. Bernhard, P. W. Marcy, C. E. Coleman-Smith, S. Huzurbazar, R. L. Wolpert, and S. A. Bass, *Phys. Rev. C* **91**, 054910 (2015).
- [26] J. E. Bernhard, J. S. Moreland, S. A. Bass, J. Liu, and U. Heinz, *Phys. Rev. C* **94**, 024907 (2016).
- [27] J. E. Bernhard, J. S. Moreland, and S. A. Bass, *Nat. Phys.* **15**, 1113 (2019).
- [28] D. Everett *et al.* (JETSCAPE Collaboration), *Phys. Rev. Lett.* **126**, 242301 (2021).
- [29] D. Everett *et al.* (JETSCAPE Collaboration), *Phys. Rev. C* **103**, 054904 (2021).
- [30] G. Nijs, W. van der Schee, U. Gürsoy, and R. Snellings, *Phys. Rev. Lett.* **126**, 202301 (2021).
- [31] G. Nijs, W. van der Schee, U. Gürsoy, and R. Snellings, *Phys. Rev. C* **103**, 054909 (2021).
- [32] G. Nijs and W. van der Schee, *Phys. Rev. Lett.* **129**, 232301 (2022).
- [33] J. E. Parkkila, A. Onnerstad, and D. J. Kim, *Phys. Rev. C* **104**, 054904 (2021).
- [34] J. E. Parkkila, A. Onnerstad, S. F. Taghavi, C. Mordasini, A. Bilandzic, M. Virta, and D. J. Kim, *Phys. Lett. B* **835**, 137485 (2022).
- [35] M. R. Heffernan, C. Gale, S. Jeon, and J.-F. Paquet, [arXiv:2302.09478](https://arxiv.org/abs/2302.09478).
- [36] V. Greco, C. M. Ko, and P. Levai, *Phys. Rev. Lett.* **90**, 202302 (2003).
- [37] V. Greco, C. M. Ko, and P. Levai, *Phys. Rev. C* **68**, 034904 (2003).
- [38] R. J. Fries, B. Muller, C. Nonaka, and S. A. Bass, *Phys. Rev. Lett.* **90**, 202303 (2003).
- [39] R. J. Fries, B. Muller, C. Nonaka, and S. A. Bass, *Phys. Rev. C* **68**, 044902 (2003).
- [40] R. J. Fries, V. Greco, and P. Sorensen, *Annu. Rev. Nucl. Part. Sci.* **58**, 177 (2008).
- [41] M. He, R. J. Fries, and R. Rapp, *Phys. Rev. C* **82**, 034907 (2010).
- [42] D. Teaney, *Phys. Rev. C* **68**, 034913 (2003).
- [43] A. Jaiswal and V. Koch, [arXiv:1508.05878](https://arxiv.org/abs/1508.05878).
- [44] Z. Yang and R. J. Fries, *J. Phys.: Conf. Ser.* **832**, 012056 (2017).
- [45] Z. Yang and R. J. Fries, [arXiv:2007.11777](https://arxiv.org/abs/2007.11777).
- [46] Z. Yang and R. J. Fries, *Phys. Rev. C* **105**, 014910 (2022).
- [47] A. Shor, *Phys. Rev. Lett.* **54**, 1122 (1985).
- [48] H. van Hecke, H. Sorge, and N. Xu, *Phys. Rev. Lett.* **81**, 5764 (1998).
- [49] L.-W. Chen and C. M. Ko, *Phys. Rev. C* **73**, 044903 (2006).
- [50] J. H. Chen, F. Jin, D. Gangadharan, X. Z. Cai, H. Z. Huang, and Y. G. Ma, *Phys. Rev. C* **78**, 034907 (2008).
- [51] J. Auvinen, K. Redlich, and S. A. Bass, *J. Phys.: Conf. Ser.* **779**, 012045 (2017).
- [52] R. C. Hwa and L. Zhu, *J. Phys.: Conf. Ser.* **779**, 012049 (2017).
- [53] Y. J. Ye, J. H. Chen, Y. G. Ma, S. Zhang, and C. Zhong, *Chin. Phys. C* **41**, 084101 (2017).
- [54] J. Pu, K.-J. Sun, and L.-W. Chen, *Phys. Rev. C* **98**, 064905 (2018).
- [55] J. Song, F.-l. Shao, and Z.-t. Liang, *Phys. Rev. C* **102**, 014911 (2020).
- [56] F. Retiere and M. A. Lisa, *Phys. Rev. C* **70**, 044907 (2004).
- [57] M. Damodaran, D. Molnar, G. G. Barnaföldi, D. Berényi, and M. Ferenc Nagy-Egri, [arXiv:1707.00793](https://arxiv.org/abs/1707.00793).
- [58] G. S. Denicol, S. Jeon, and C. Gale, *Phys. Rev. C* **90**, 024912 (2014).
- [59] J.-F. Paquet, C. Shen, G. S. Denicol, M. Luzum, B. Schenke, S. Jeon, and C. Gale, *Phys. Rev. C* **93**, 044906 (2016).
- [60] B. Nerlo-Pomorska and K. Pomorski, *Z. Phys. A* **348**, 169 (1994).
- [61] B. Abelev *et al.* (ALICE Collaboration), *Phys. Rev. C* **88**, 044909 (2013).

- [62] J. Adamczewski-Musch *et al.* (HADES Collaboration), *Eur. Phys. J. A* **54**, 85 (2018).
- [63] J. Adams *et al.* (STAR Collaboration), *Phys. Rev. Lett.* **98**, 062301 (2007).
- [64] B. I. Abelev *et al.* (STAR Collaboration), *Phys. Rev. Lett.* **99**, 112301 (2007).
- [65] L. Adamczyk *et al.* (STAR Collaboration), *Phys. Rev. Lett.* **116**, 062301 (2016).
- [66] B. B. Abelev *et al.* (ALICE Collaboration), *Phys. Lett. B* **728**, 216 (2014); Erratum *ibid.* **734**, 409 (2014).
- [67] B. B. Abelev *et al.* (ALICE Collaboration), *J. High Energy Phys.* **06** (2015) 190.
- [68] J. Adam *et al.* (ALICE Collaboration), *Phys. Rev. C* **95**, 064606 (2017).
- [69] P. Huovinen and P. Petreczky, *Nucl. Phys. A* **837**, 26 (2010).
- [70] S. A. Bass *et al.* (MADAI Collaboration) <http://madai.phy.duke.edu/>, accessed June 2016.
- [71] A. Dash, S. Samanta, and B. Mohanty, *Phys. Rev. D* **100**, 014025 (2019).
- [72] J. Noronha-Hostler, J. Noronha, and C. Greiner, *Phys. Rev. Lett.* **103**, 172302 (2009).
- [73] J. B. Rose, J. M. Torres-Rincon, and H. Elfner, *J. Phys. G: Nucl. Part. Phys.* **48**, 015005 (2021).
- [74] J. Auvinen, K. J. Eskola, P. Huovinen, H. Niemi, R. Paatelainen, and P. Petreczky, *Phys. Rev. C* **102**, 044911 (2020).
- [75] V. Mykhaylova, M. Bluhm, K. Redlich, and C. Sasaki, *Phys. Rev. D* **100**, 034002 (2019).
- [76] W. Zhao, C. M. Ko, Y.-X. Liu, G.-Y. Qin, and H. Song, *Phys. Rev. Lett.* **125**, 072301 (2020).